

# Numerical Analysis of the Flow in a Delayed Coker Unit Fractionator Overhead Vapor Line

Chun-Lang Yeh

**Keywords :** delayed coker unit, computational fluid dynamics, fractionator, force uniformity.

## ABSTRACT

In this study, we applied computational fluid dynamics (CFD) to investigate the flow in a delayed coker unit (DCU) fractionator overhead vapor line connected to an air cooler. The causes of the pipe damage and the strategies to alleviate the occurrence of the damage are discussed. It is found that the flow direction of the working fluid in the 30" main pipe biases the downstream flow to the east side, which causes the east half part of the pipe system to deteriorate earlier than the west half part due to the larger erosion effect. Raising the 30" pipe does not improve the force uniformity. If the two 24" pipes are connected and the five 18" pipes are also connected, the force uniformity can be improved without raising the 30" pipe. In addition, the forces on caps, reducers and T-junctions all reduce if the two 24" pipes are connected and the five 18" pipes are also connected.

## INTRODUCTION

Delayed coking is a major process operation in an oil refinery. It is used to thermally crack high molecular weight feed-stocks, normally vacuum tar from the vacuum unit, into sour gas, naphtha, light gas oil, heavy gas oil and coke. A delayed coker unit consists of a fractionator, a furnace and at least two coke drums, as shown in Fig. 1. Only one coke drum is onstream at a time while the others are in some stage of decoking or preheating in preparation for the next cycle. The switching of the coke drums severely destabilizes the operation of the fractionator and downstream process units (Hsu and Robinson, 2019; Depew, Hashemi, and Davis, 1988).

The fresh feedstocks are heated and then introduced into the fractionator bottom to quench the

superheated reacting vapors. The preheated feedstocks from the fractionator bottom, together with the condensed heavier ends from the reacting vapors, is pumped into the radiation section of the furnace and quickly heated. After partially vaporized in the heater tubes, the feedstocks are introduced into one of the two coke drums where the coking reactions take place. High pressure water is then injected into the furnace tubes to minimize the coke deposition and to delay the coking reactions in the tubes. The superheated reacting vapors from the top of the coke drums are then drawn back to the fractionator base and are further separated into various products such as wet gas, naphtha, light gas oil, and heavy gas oil, according to their boiling points. The coker fractionator overhead vapor is cooled in the fractionator overhead air cooler (Abdul Rahman, 2009).

Depew, Hashemi, and Davis (1988) proposed a rigorous process model to simulate the DCU operation. The simulation results are used to evaluate various control strategies. Kedia, Nallasivam, and Ambati (2019) developed an approach to numerically estimate the percentage reduction in standard deviation of the key controlled process variables. The effectiveness of the method is justified by implementing it in MATLAB on real process plant data of the DCU in a petrochemical refinery which experiences cyclic disturbance. Zhang and Yu (1999) built multiple variables model of the liquid products of a delayed coking plant via RBF (Radial Basis Function) neural networks. The model provides yield ratio of gasoline, diesel oil, coker gas-oil and general yield ratio of liquid products simultaneously. Chen and Wang (2020) used the n-d-M method, E-d-M method and hydrocarbon group analysis method to analyze the composition and properties of the delayed coker feedstocks (vacuum residue, FCC (Fluidized Catalytic Cracking) slurry) and ethylene tar. Their results showed that blending ethylene tar in the delayed coker feedstock would lead to a decrease in the saturation and an increase in the aromatic content of the feedstock. Lei et al. (2015) established an integrated optimization model based on stage-wise superstructure of heat exchanger networks, taking heat removals from the complex fractionator as key coupling variables. Results of three optimization

*Paper Received September, 2023. Revised November, 2023. Accepted December, 2023. Author for Correspondence: Chun-Lang Yeh.*

*Professor, Department of Aeronautical Engineering, National Formosa University, Yunlin, Taiwan 63208, ROC.*

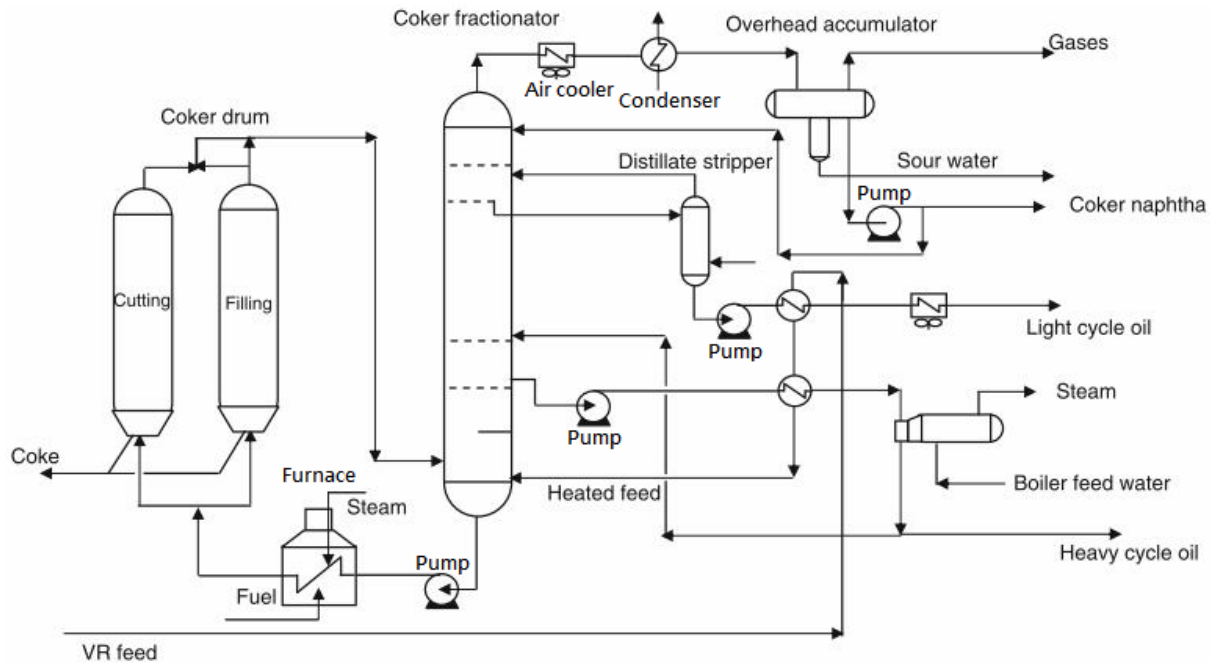


Fig. 1. Illustration of a Delayed Coker Unit.

levels were compared in the case study. The authors indicated that it is superior to consider steam generation in integrated optimization. Ge Xin (2022) solved the difficult problem of mixed waste oil by optimizing the technological process and analyzing the effect after putting into use. The results showed that the yield of diesel increased by 2.59% after refining the mixed waste oil. Deng, Cai and Li (2022) solved the usage problem of catalytic cracking slurry by carrying out the test of high-proportion blending of catalytic cracking slurry. The results showed that when the blending ratio of catalytic cracking slurry increased from 25% to 29%, the yield of petroleum coke decreased significantly, the yield of gas oil increased, and the yield of light oil and total liquid increased. Fan et al. (2022) applied a heat load automatic adjustment simulation method for three-point steam injection in a delayed coker furnace. The influence of three-point steam injection rate on the coking degree and heat consumption was analyzed. The results showed that the rate of steam injection affected the heat consumption and the coking degree. Improving the steam injection rate would increase the heat consumption and decrease the coking degree at the same time. Paladino et al. (2005) developed a CFD model for the washing zone, including the vapor (feed) and the washing liquid, considering the heat and mass transfer between phases, to be able to predict the necessary height for the vapor to reach the required temperature and to avoid the coke formation in this region. The model could reproduce the complex phenomena of interfacial heat and mass transfer on multi-component multiphase flows. Díaz et al. (2017) applied CFD to simulate a pilot plant delayed coking reactor. The

cooling of the resulting coke bed for three different vacuum residues were simulated and the results were compared with experimental data. Ibrahim et al. (2022) performed a computer simulation and salutory analysis for two types of crude oil to reach the goal of the ideal mixing ratio between the heavy crude to be used as a substitute for crude oil in the delayed coke production unit. Based on the results of laboratory testing, computer simulations and lab analysis performed, blending 50% of DAR blend with 50% of Fula blend ore in the delayed coke production unit achieved a good improvement in the specifications and quantities of the products. Albers (1996) develop models to improve the ability of predicting yields and quality. Three different modeling approaches that have been tried use kinetic, Monte Carlo, and empirical techniques. The models were used to improve the control and optimization of the delayed coking process. Valenca, Waturuocha and Wisecarver (2015) performed a 2D axisymmetric simulation of a pilot coke drum that receives nitrogen gas to check restrictions in the flow lines and to pre-heat the unit at a given temperature among other safety and process reasons. The results show that the model predicts a linear trend for the temperature profile as obtained in the experimental run. Mohamed et al. (2022) built a simulation model using Aspen HYSYS to obtain results and to make an optimization for the process variables of the delayed coker unit while comparing them to the old design case to achieve the maximum gas oil yield while keeping process safety factors in concerns.

Most of the existing DCU researches are relevant to the optimization of DCU process variables to achieve better product yields. There were very few studies relevant to the investigation of the DCU pipe damage, which is closely connected with the

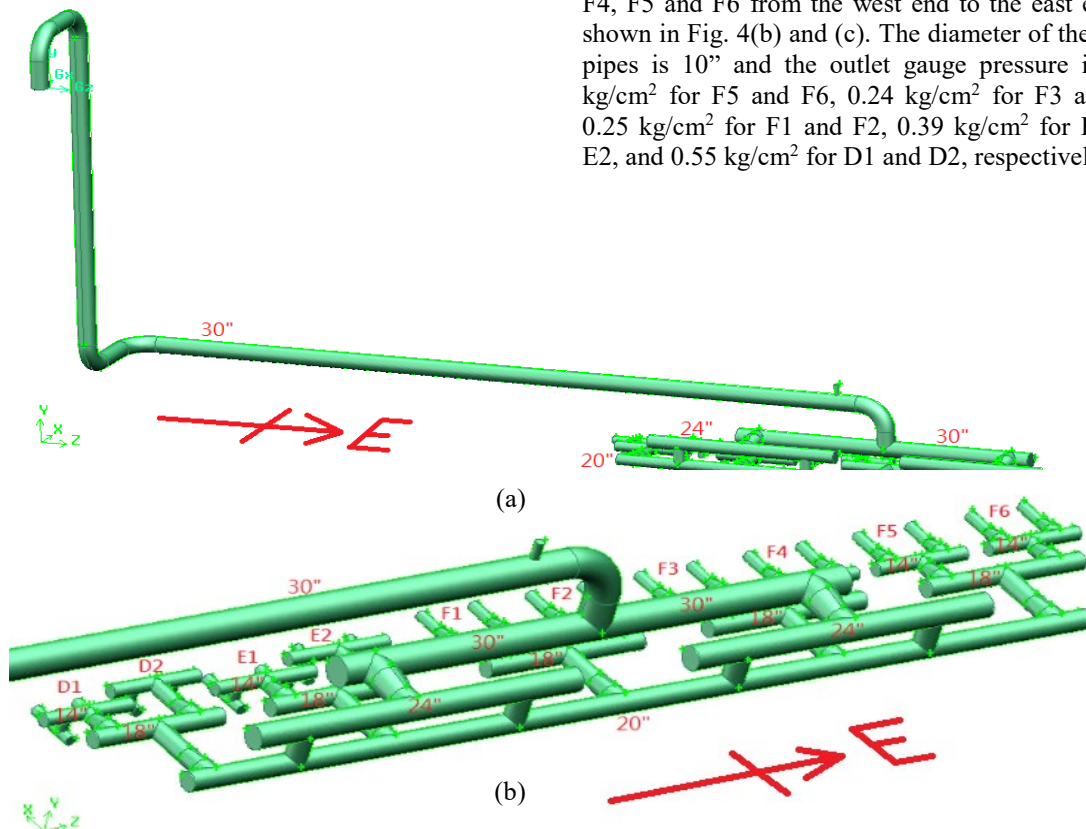
equipment operation safety and service life. In this paper, we applied CFD to study the flow in a practical DCU fractionator overhead vapor line connected to an air cooler, as shown in Fig. 2. Because of the complex geometry and flow development in the pipe system, damages of the pipe have been found. For example, Fig. 3(a) shows the leakage near a T-junction in the east half part of the pipe system. Another example shown in Fig. 3(b) is the pipe wall thickness near a T-junction, reducer and cap in the east half part of the pipe system which has become thinner. This paper discussed the causes of the damage and the strategies to alleviate the occurrence of the damage.



Fig. 2. A practical fractionator overhead vapor line.



Fig. 3. Two damages in the fractionator overhead vapor line shown in Fig. 2.

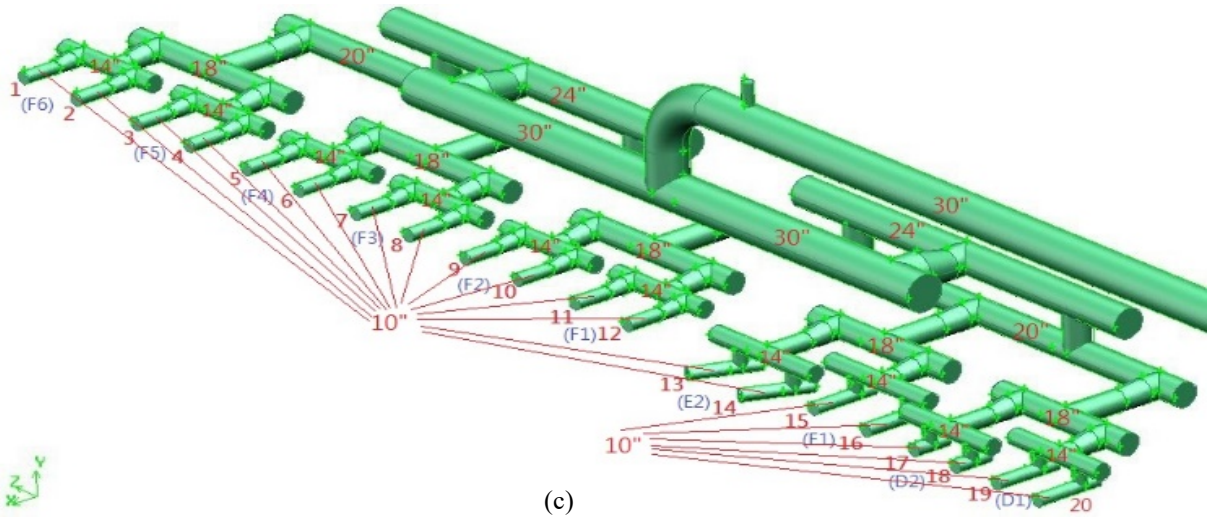


## NUMERICAL METHODS

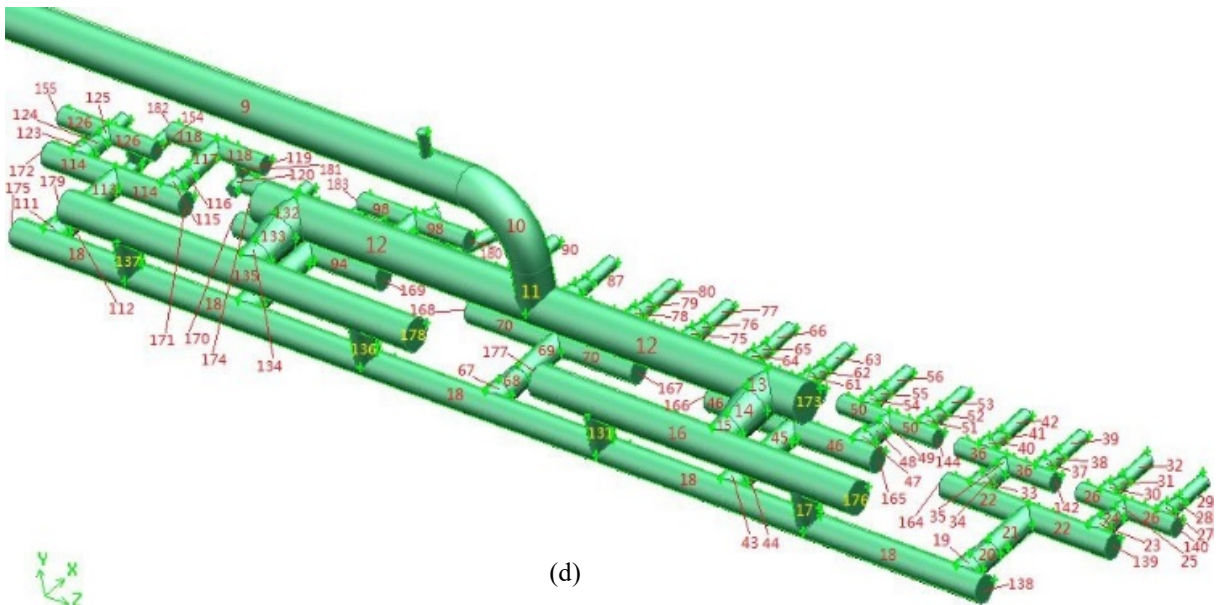
In this study, the ANSYS FLUENT commercial code (Fluent Inc., 2017) is employed to simulate the fluid flow in the pipeline. The SIMPLE algorithm by Patankar (1980) is used to solve the governing equations. The discretizations of convection terms and diffusion terms are carried out by the power-law scheme and the central difference scheme, respectively. In respect of physical models, by considering the accuracy and stability of the models, the standard  $k-\epsilon$  Model (Launder and Spalding, 1972) is adopted for turbulence simulation. The standard wall functions (Launder and Spalding, 1974) are used to resolve the flow quantities, including velocity and turbulence quantities, at the near-wall regions.

Fig. 4 shows the model for the practical fractionator overhead vapor line connected to the air cooler shown in Fig. 2. We test five different mesh sizes: 0.5m, 0.1m, 0.064m, 0.04m, and 0.032m. The difference between the maximum force acting on the pipe system obtained from mesh sizes of 0.04m and 0.032m is within 0.5%. Therefore, the mesh size of 0.032m is used for the subsequent discussion. The number of mesh volumes generated by the mesh size of 0.032m is around four million, which is close to the maximum number of mesh volumes we can generate in our workstation with 128G ram.

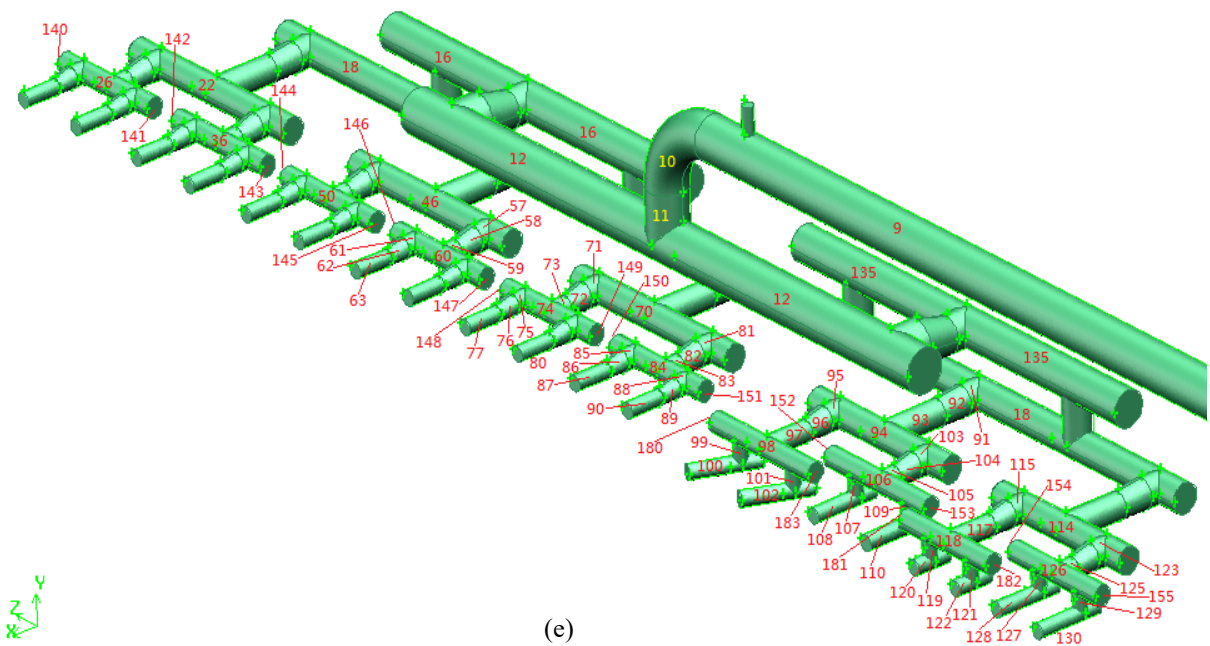
The diameter of the inlet pipe is 30". The inlet velocity and gauge pressure are 32.93 m/sec and 0.6 kg/cm<sup>2</sup>, respectively. The 20 outlet pipes are divided into 10 bundles, including D1, D2, E1, E2, F1, F2, F3, F4, F5 and F6 from the west end to the east end, as shown in Fig. 4(b) and (c). The diameter of the outlet pipes is 10" and the outlet gauge pressure is 0.19 kg/cm<sup>2</sup> for F5 and F6, 0.24 kg/cm<sup>2</sup> for F3 and F4, 0.25 kg/cm<sup>2</sup> for F1 and F2, 0.39 kg/cm<sup>2</sup> for E1 and E2, and 0.55 kg/cm<sup>2</sup> for D1 and D2, respectively. The



(c)



(d)



(e)

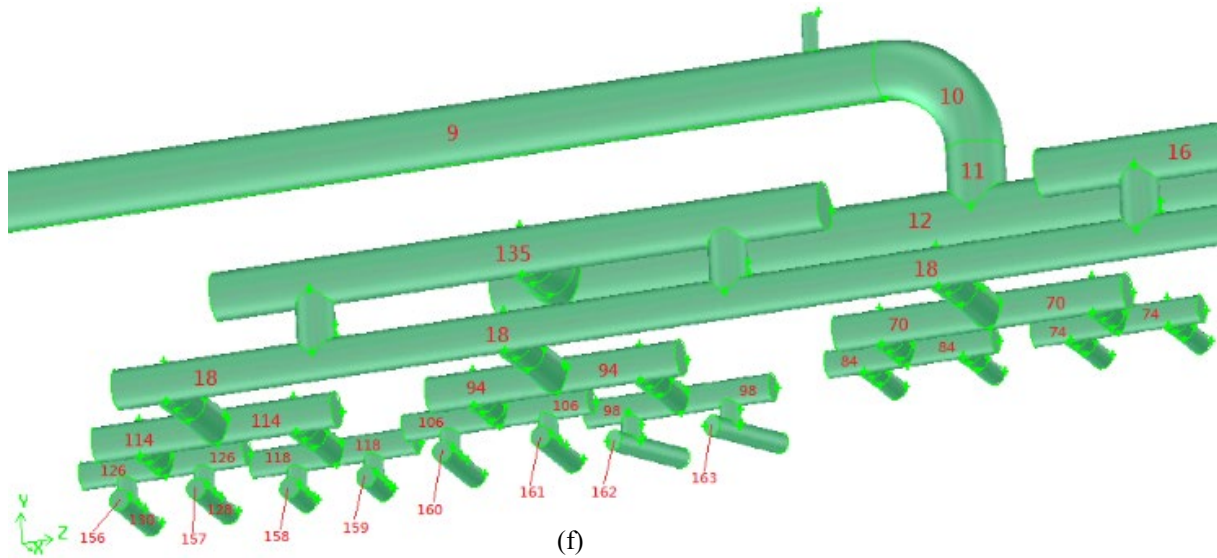


Fig. 4. Model for the practical fractionator overhead vapor line shown in Fig. 2 and the positions on the pipe system corresponding to the results shown in Fig.5 and Table 1 to Table 5.

working fluid is water vapor at 129°C. The turbulence kinetic energy ( $m^2/s^2$ ) at the pipe inlet is assumed to be 10% of the inlet mean flow kinetic energy and the corresponding turbulence kinetic energy dissipation rate ( $m^2/s^3$ ) is computed from the following empirical relation:

$$\varepsilon = C_{\mu}^{3/4} \frac{k^{3/2}}{l} \quad (1)$$

where  $C_{\mu}=0.09$ ,  $l=0.07L$  and  $L$  is the hydraulic diameter (m).

## RESULTS AND DISCUSSION

### Flow Asymmetry of the Pipe System

For the real pressure distribution, the flow is biased to the east side. This phenomenon results from the flow direction of the working fluid in the 30" main pipe. As can be seen from Fig. 4, the fluid in the 30" pipe flows from the west side to the east side. Therefore, the downstream fluid tends to flow toward the east side from Newton's first law of motion (law of inertia). This result causes the east half part of the pipe system to deteriorate earlier than the west half part due to the larger erosion effect. Two examples are shown in Fig. 3. To remedy this, the pipe system should be changed so that the bias of the flow can be alleviated. For example, the designed outlet gauge pressure of the pipe system is 0.34 kg/cm<sup>2</sup> from Fig. 13.2 of ASME SEC.VIII DIV.1 APPENDIX 13 (ASME, 2023). If this designed outlet gauge pressure is used, the mass flow rate distribution for the pipe system at the exit shown in Fig.4(c) is much more uniform, as can be seen from Fig. 5.

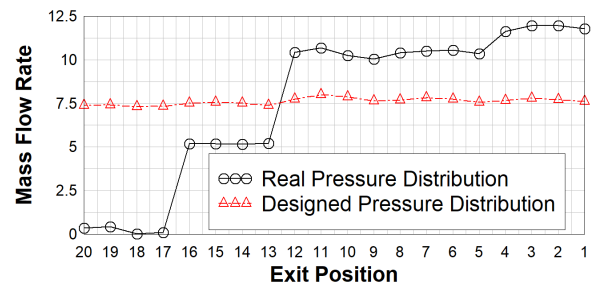


Fig. 5. Distribution of mass flow rate for real and designed pressure distribution.

### Force Uniformity of the Pipe System

The flow asymmetry is closely connected with the uniformity of the force on the pipe system. To compare the effectiveness of the pipe system improvement, the uniformity of the force should be inspected in addition to the force on the pipe system. For  $n$  variables,  $f_1, f_2, \dots, f_n$ , a uniformity index is defined as

$$\gamma = (|f_1 - \bar{f}| + |f_2 - \bar{f}| + |f_3 - \bar{f}| + \dots + |f_n - \bar{f}|) / n \quad (2)$$

where  $\bar{f}$  is the average of  $f_1, f_2, \dots, f_n$ , i.e.  $\bar{f} = (f_1 + f_2 + f_3 + \dots + f_n) / n$ . The uniformity index represents the deviation of the variables from their average. A smaller uniformity index implies better uniformity. In the following discussion, we attempt to change the arrangement of the pipe system so that the flow uniformity can be improved.

In CFD flow simulation, boundary conditions have significant influence on the simulation results. The inlet boundary condition (velocity, pressure, and turbulence quantities) has been stated above. The pressure outlet of FLUENT is adopted as the outlet boundary condition. In this study, we consider two outlet pressure distributions. The first is the measured

gauge pressure values: 0.19 kg/cm<sup>2</sup> for F5 and F6, 0.24 kg/cm<sup>2</sup> for F3 and F4, 0.25 kg/cm<sup>2</sup> for F1 and F2, 0.39 kg/cm<sup>2</sup> for E1 and E2, and 0.55 kg/cm<sup>2</sup> for D1 and D2, respectively. The second is the designed outlet gauge pressure value 0.34 kg/cm<sup>2</sup> derived from Fig. 13.2 of ASME SEC.VIII DIV.1 APPENDIX 13. Note that the average of the measured outlet gauge pressure values is close to the designed outlet gauge pressure value. If the non-uniformity of the flow in the pipe system is improved, the measured outlet gauge pressure values should approach the designed outlet gauge pressure value. In the following discussion, we investigate five cases of pipe arrangement and boundary conditions.

Case 1: Current pipe arrangement and measured outlet gauge pressure values.

Case 2: Current pipe arrangement and designed outlet gauge pressure value.

Case 3: The two 24" pipes are connected and the five 18" pipes are also connected. Designed outlet gauge pressure value is used.

Case 4: The 30" pipe is raised by 9m. Designed outlet gauge pressure value is used.

Case 5: The 30" pipe is raised by 4m. The two 24" pipes are connected and the five 18" pipes are also connected. Designed outlet gauge pressure value is used.

The purpose of comparing the above five cases includes the following two reasons.

1. The pipe arrangements of Case 3, 4 and 5 basically improve the flow uniformity and hence the outlet pressure becomes more uniform. Therefore, designed outlet gauge pressure is used instead of measured outlet gauge pressures.
2. The current pipe arrangement results in the bias of the downstream flow to the east side and hence the outlet pressure distribution is rather non-uniform. Therefore, comparing Case 1 with Case 3, 4 and 5 which pipe arrangements have been improved is not suitable. A more reasonable way is to fix the outlet pressure distribution and then compare the effectiveness of the pipe arrangement before and after improvement. Therefore, Case 2 use current pipe arrangement and the designed outlet gauge pressure. The results of Case 2, 3, 4 and 5 are then compared to investigate the effectiveness of the pipe arrangement before and after improvement. Table 1 shows the comparison of force (sum of pressure force and viscous force) uniformity for Case 1 to Case 5. From Table 1, we deduce the following three points.
  1. In Table 1, the red number in Case 2 means the uniformity of Case 2 worse than that of Case 1. It can be observed that Case 2 is more uniform than Case 1.
  2. The brown number in Case 3, the green number in Case 4, and the blue number in Case 5 represent their uniformity worse than that of Case 2. It can

be observed that Case 3 is the most uniform case and Case 5 is the next. Both Case 3 and Case 5 are more uniform than Case 2. Case 4 and Case 2 are equally uniform, which means that raising the 30" pipe by 9m does not improve the force uniformity. This may be caused by the transformation of potential energy into kinetic energy at the 30" T-junction which lead to a slower flow rectification. If the 30" pipe is horizontally elongated and connected to the 30" T-junction, the uniformity may be improved. However, the 30" pipe cannot be horizontally elongated and connected to the 30" T-junction due to the limitation of available space. To make sure the above results, other raising height will be discussed later.

3. In Table 1, the red number in the RHS column (Case 5) represents the uniformity of Case 5 worse than that of Case 3. It can be observed that Case 3 is more uniform than Case 5, which means that if the two 24" pipes are connected and the five 18" pipes are also connected, the force uniformity can be improved without raising the 30" pipe. To make sure the above results, other raising height will be discussed later.

From the above discussion, we can see that raising the 30" pipe by 9m does not improve the force uniformity. To make sure the above observation, other raising height, including 1m, 2m, 3m, 4m, 5m, 6m, 7m and 8m, are discussed. In Table 2, the two 24" pipes are connected and the five 18" pipes are also connected. The 30" pipe is raised by the height listed in Table 2. The designed outlet gauge pressure is used. In Table 2, the red number represents the uniformity worse than that of raising height 9m. It can be observed that raising height of 4m (corresponding to Case 5 in Table 1) is the most uniform case. However, from Table 1, Case 3 is more uniform than Case 5, which confirms that if the two 24" pipes are connected and the five 18" pipes are also connected, the force uniformity can be improved without raising the 30" pipe.

### Force on the Pipe System

To compare the force on the pipe system for different pipe arrangement and boundary conditions, we investigate the following three cases:

Case 1: Current pipe arrangement and measured outlet gauge pressure values.

Case 2: The two 24" pipes are connected and the five 18" pipes are also connected. Measured outlet gauge pressure value is used.

Case 3: The two 24" pipes are connected and the five 18" pipes are also connected. Designed outlet gauge pressure value is used.

From the simulation results, it is found that the positions subjected to larger forces include caps, reducers and T-junctions. Table 3 shows the

Table 1. Force uniformity for Case 1 to Case 5.

Wall position		Case 1	Case 2	Case 3	Case 4	Case 5	Case 5
30" to 24"	13,132	0.156	2.24E-02	5.20E-03	2.07E-02	1.03E-02	1.03E-02
	14,133	0.108	0.00E+00	4.06E-04	2.71E-04	4.06E-04	4.06E-04
	15,134	1.80E-02	1.78E-02	8.57E-02	2.01E-02	2.27E-02	2.27E-02
20" to 18"	19,43,67,91,111	0.496	0.459	0.421	0.456	0.374	0.374
	20,44,68,92,112	0.185	3.61E-03	2.96E-03	3.84E-03	3.11E-03	3.11E-03
	21,45,69,93,113	0.431	0.108	0.121	0.112	0.134	0.134
18" to 14"	23,33,47,57,71,81,95,103,115,123	0.384	7.46E-02	0.124	6.99E-02	0.150	0.150
	24,34,48,58,72,82,96,104,116,124	0.196	2.27E-03	1.75E-03	2.39E-03	1.86E-03	1.86E-03
	25,35,49,59,73,83,97,105,117,125	0.503	0.285	0.284	0.286	0.283	0.283
14" to 10"	27,30,37,40,51,54,61,64,75,78,85,88	0.105	6.32E-02	5.43E-02	6.21E-02	7.08E-02	7.08E-02
	28,31,38,41,52,55,62,65,76,79,86,89	6.01E-02	5.41E-04	4.81E-04	5.36E-04	5.03E-04	5.03E-04
	29,32,39,42,53,56,63,66,77,80,87,90	9.01E-02	7.47E-02	5.32E-02	7.05E-02	7.34E-02	7.34E-02
14" to 10"	107,109,127,129	0.565	0.120	4.01E-02	0.114	0.127	0.127
	108,110,128,130	0.112	1.03E-03	9.55E-04	8.08E-04	8.45E-04	8.45E-04
14" to 10"	99,101	0.443	0.358	0.243	0.322	0.275	0.275
	100,102	4.48E-03	2.93E-04	4.40E-04	4.39E-04	1.47E-04	1.47E-04
14" to 10"	119,121	4.51E-02	4.55E-02	4.12E-02	3.22E-02	4.99E-02	4.99E-02
	120,122	1.43E-04	2.31E-04	0.00E+00	3.85E-04	2.31E-04	2.31E-04
30" Cap	173,174	4.91E-02	1.51E-04	1.51E-04	7.54E-05	1.51E-04	1.51E-04
24" Cap	176,177,178,179	8.59E-02	6.53E-04	3.84E-04	8.84E-04	1.54E-04	1.54E-04
20" Cap	138,175	0.176	3.37E-03	3.60E-03	3.52E-03	3.13E-03	3.13E-03
18" Cap	139,164,165,166,167,168,169,170,171,172	0.174	1.99E-03	2.22E-03	2.23E-03	2.38E-03	2.38E-03
14" Cap	140,141,142,143,144,145,146,147,148,149,150,151,152,153,154,155	0.162	3.27E-03	3.13E-03	3.38E-03	3.05E-03	3.05E-03
14" Cap	180,183,181,182	0.103	5.57E-04	1.99E-04	2.39E-04	1.99E-04	1.99E-04
10" Cap	161,160,157,156	0.136	4.82E-04	5.62E-04	4.01E-04	4.01E-04	4.01E-04
10" Cap	163,162,159,158	0.143	1.40E-04	1.20E-04	3.21E-04	2.41E-04	2.41E-04

comparison of forces (per unit area due to pressure force and viscous force) on the caps subjected to larger forces, Table 4 shows the comparison of forces on the reducers subjected to larger forces and Table 5 shows the comparison of forces on the T-junctions subjected to larger forces. From Table 3, it is observed that among the 26 caps subjected to larger forces, there are 9 positions that forces of Case 2 are

higher than those of Case 1, while there are 17 positions that forces of Case 1 are higher than those of Case 2. From Table 4, it is observed that among the 29 reducers subjected to larger forces, there are 13 positions that forces of Case 2 are higher than those of Case 1, while there are 16 positions that forces of Case 1 are higher than those of Case 2. From Table 5, it is observed that among the 13

Table 2. Force uniformity for different raising height.

Wall position	1m	2m	3m	4m(Case5)	5m	6m	7m	8m	9m	
30" to 24"	13,132	1.20E-02	2.64E-02	1.09E-02	1.03E-02	1.43E-2	9.40E-03	8.66E-03	2.25E-03	6.88E-03
	14,133	4.74E-04	6.09E-04	3.39E-04	4.06E-04	3.39E-4	4.06E-04	3.39E-04	2.71E-04	4.06E-04
	15,134	3.36E-02	4.15E-02	4.01E-02	2.27E-02	4.67E-2	5.54E-02	4.97E-02	7.51E-02	4.12E-02
20" to 18"	19,43,67,91,111	0.304078	0.420	0.377	0.374271	0.380	0.444	0.387	0.429	0.417
	20,44,68,92,112	2.93E-03	2.93E-03	3.06E-03	3.11E-03	3.06E-03	3.26E-03	2.86E-03	3.06E-03	3.11E-03
18" to 14"	21,45,69,93,113	0.153	0.156	0.150	0.134	0.148	0.105	0.149	0.160	0.143
	23,33,47,57,71,81,95,103,115,123	0.138	0.133	0.159	0.150	0.146	0.126	0.123	0.132	0.122
	24,34,48,58,72,82,96,104,116,124	1.74E-03	1.65E-03	1.81E-03	1.86E-03	1.79E-03	1.87E-03	1.80E-03	1.94E-03	1.79E-03
14" to 10"	25,35,49,59,73,83,97,105,117,125	0.280	0.283	0.284	0.283	0.284852	0.284	0.281	0.283	0.283
	27,30,37,40,51,54,61,64,75,78,85,88	6.12E-02	5.99E-02	6.92E-02	7.08E-02	6.82E-02	6.29E-02	6.21E-02	6.53E-02	6.04E-02
	28,31,38,41,52,55,62,65,76,79,86,89	4.92E-04	4.45E-04	4.81E-04	5.03E-04	4.48E-04	5.03E-04	4.48E-04	4.72E-04	5.14E-04
14" to 10"	29,32,39,42,53,56,63,66,77,80,87,90	6.44E-02	6.08E-02	7.22E-02	7.34E-02	7.16E-02	6.31E-02	6.05E-02	6.89E-02	6.14E-02
	107,109,127,129	9.94E-02	8.33E-02	9.43E-02	0.127	7.79E-02	8.33E-02	0.102	0.109	8.45E-02
14" to 10"	108,110,128,130	8.82E-04	1.03E-03	8.08E-04	8.45E-04	7.35E-04	9.92E-04	1.03E-03	8.82E-04	7.35E-04
	99,101	0.286	0.287	0.270	0.275	0.277	0.221	0.283	0.342	0.285
14" to 10"	100,102	2.93E-04	5.86E-04	2.93E-04	1.47E-04	5.86E-04	4.40E-04	4.40E-04	4.40E-04	1.47E-04
	119,121	5.43E-02	4.55E-2	3.06E-02	4.99E-02	6.10E-02	2.75E-02	1.78E-02	3.96E-02	3.62E-02
14" to 10"	120,122	3.08E-04	2.31E-4	2.31E-04	2.31E-04	7.71E-05	2.31E-04	7.71E-05	0.00E+00	3.08E-04
	173,174	1.51E-04	2.26E-04	2.26E-04	1.51E-04	2.26E-04	1.51E-04	7.54E-05	7.55E-05	1.51E-04
24" Cap	176,177,178,179	7.68E-05	2.30E-04	1.54E-04	1.54E-04	2.30E-04	4.61E-04	3.84E-04	4.61E-04	3.84E-04
20" Cap	138,175	2.43E-03	3.44E-03	3.21E-03	3.13E-03	3.45E-03	3.76E-03	2.90E-03	3.68E-03	3.60E-03
18" Cap	139,164,165,166,167,168,169,170,171,172	2.38E-03	2.14E-03	2.22E-03	2.38E-03	2.30E-03	2.46E-03	2.38E-03	2.54E-03	2.22E-03
14" Cap	140,141,142,143,144,145,146,147,148,149,150,151,152,153,154,155	3.01E-03	3.16E-03	3.00E-03	3.05E-03	3.14E-03	3.32E-03	3.28E-03	3.17E-03	3.09E-03
14" Cap	180,183,181,182	2.99E-04	2.19E-04	2.79E-04	1.99E-04	1.59E-04	1.99E-04	3.19E-04	3.78E-04	2.39E-04
10" Cap	161,160,157,156	3.81E-04	5.22E-04	4.01E-04	4.01E-04	3.81E-04	5.22E-04	5.62E-04	4.01E-04	3.61E-04
10" Cap	163,162,159,158	2.41E-04	3.21E-04	2.01E-04	2.41E-04	2.01E-04	2.81E-04	2.01E-04	2.41E-04	2.81E-04

T-junctions subjected to larger forces, there are 6 positions that forces of Case 2 are higher than those of Case 1, while there are 7 positions that forces of Case 1 are higher than those of Case 2. From the above comparisons, it can be seen that if the two 24" pipes are connected and the five 18" pipes are also connected, the forces on the caps, reducers and T-junctions all reduce. It should be noted that, in Case 2, the two 24" pipes are connected and the five 18" pipes are also connected but measured outlet gauge pressure values are used. This is unreasonable for Case 2 because the flow uniformity should be better if the two 24" pipes are connected and the five 18" pipes are also connected. This can be deduced from the force uniformity discussed in Table 1 and the force listed in Table 3, 4 and 5. In practice, if the two

24" pipes are connected and the five 18" pipes are also connected, the outlet pressures should be more uniform than the measured pressure distribution and the forces should be lower than those of Case 2 listed in Table 3, 4 and 5. Case 3 also reveals this. For Case 3, the two 24" pipes are connected and the five 18" pipes are also connected. Designed outlet gauge pressure is used. From Table 3, 4 and 5, it can be observed that among the 68 positions (including caps, reducers and T-junctions) subjected to larger forces, there are only 6 positions that forces of Case 3 are higher than those of Case 1, while there are 62 positions that forces of Case 1 are higher than those of Case 3. From this result, if the outlet pressure distributions of Case 2 become more uniform, the forces of Case 2 should be lower than those of Case 2

listed in Table 3, 4 and 5, even if they cannot be as low as Case 3.

Table 3. Comparison of force (Nt/m<sup>2</sup>) on the caps subjected to larger forces.

Position	Case 1	Case 2	Case 3
Wall141	0.7637E+05	0.7627E+05	0.6226E+05
Wall142	0.7636E+05	0.7621E+05	0.6231E+05
Wall143	0.7636E+05	0.7622E+05	0.6227E+05
Wall140	0.7635E+05	0.7624E+05	0.6225E+05
Wall139	0.7523E+05	0.7425E+05	0.6285E+05
Wall164	0.7523E+05	X	X
Wall173	0.7434E+05	0.7534E+05	0.6633E+05
Wall138	0.7414E+05	0.7362E+05	0.6367E+05
Wall174	0.7381E+05	0.7533E+05	0.6631E+05
Wall176	0.7376E+05	0.7419E+05	0.6510E+05
Wall177	0.7368E+05	X	X
Wall165	0.7216E+05	X	X
Wall166	0.7203E+05	X	X
Wall144	0.7180E+05	0.7195E+05	0.6225E+05
Wall145	0.7180E+05	0.7188E+05	0.6231E+05
Wall146	0.7179E+05	0.7159E+05	0.6234E+05
Wall147	0.7177E+05	0.7159E+05	0.6228E+05
Wall178	0.7172E+05	X	X
Wall179	0.7160E+05	0.7378E+05	0.6515E+05
Wall167	0.7066E+05	X	X
Wall168	0.7065E+05	X	X
Wall148	0.7063E+05	0.7110E+05	0.6226E+05
Wall149	0.7063E+05	0.7095E+05	0.6233E+05
Wall150	0.7063E+05	0.7046E+05	0.6240E+05
Wall151	0.7062E+05	0.7048E+05	0.6230E+05
Wall175	0.6855E+05	0.7100E+05	0.6413E+05

Table 4. Comparison of force (Nt/m<sup>2</sup>) on the reducers subjected to larger forces.

Position	Case 1	Case 2	Case 3
Wall024	0.9857E+04	0.9701E+04	0.8205E+04
Wall034	0.9856E+04	0.9634E+04	0.8221E+04
Wall048	0.9459E+04	0.9442E+04	0.8210E+04
Wall058	0.9447E+04	0.9403E+04	0.8226E+04
Wall031	0.9384E+04	0.9355E+04	0.7623E+04
Wall041	0.9381E+04	0.9339E+04	0.7619E+04
Wall038	0.9380E+04	0.9336E+04	0.7623E+04
Wall028	0.9377E+04	0.9344E+04	0.7620E+04
Wall072	0.9287E+04	0.9308E+04	0.8210E+04
Wall082	0.9286E+04	0.9080E+04	0.8230E+04
Wall062	0.8822E+04	0.8813E+04	0.7626E+04
Wall052	0.8821E+04	0.8829E+04	0.7618E+04
Wall055	0.8821E+04	0.8820E+04	0.7627E+04
Wall065	0.8820E+04	0.8814E+04	0.7620E+04
Wall076	0.8695E+04	0.8718E+04	0.7618E+04
Wall079	0.8695E+04	0.8696E+04	0.7628E+04
Wall086	0.8695E+04	0.8651E+04	0.7630E+04
Wall089	0.8694E+04	0.8658E+04	0.7618E+04

Wall014	0.8361E+04	0.8411E+04	0.7392E+04
Wall096	0.8158E+04	0.8498E+04	0.8237E+04
Wall133	0.8148E+04	0.8406E+04	0.7386E+04
Wall104	0.8113E+04	0.8035E+04	0.8257E+04
Wall124	0.7172E+04	0.7604E+04	0.8245E+04
Wall116	0.7114E+04	0.8081E+04	0.8247E+04
Wall020	0.3690E+04	0.3681E+04	0.3147E+04
Wall044	0.3582E+04	0.3635E+04	0.3162E+04
Wall068	0.3531E+04	0.3588E+04	0.3169E+04
Wall092	0.3162E+04	0.3463E+04	0.3181E+04
Wall112	0.3025E+04	0.3328E+04	0.3172E+04

Table 5. Comparison of force (Nt/m<sup>2</sup>) on the T-junctions subjected to larger forces.

Position	Case 1	Case 2	Case 3
Wall036/037	0.3482E+04	0.3500E+04	0.2776E+04
Wall036/040			
Wall026/027	0.3481E+04	0.3494E+04	0.2777E+04
Wall026/030			
Wall060/061	0.3235E+04	0.3244E+0	0.2775E+04
Wall060/064			
Wall050/051	0.3234E+04	0.3227E+04	0.2776E+04
Wall050/054			
Wall084/085	0.3199E+04	0.3215E+04	0.2773E+04
Wall084/088			
Wall074/075	0.3198E+04	0.3177E+04	0.2775E+04
Wall074/078			
Wall016/017	0.2717E+04	0.2185E+04	0.1922E+04
Wall016/131			
Wall018/019	0.2716E+04	0.2769E+04	0.2446E+0
Wall018/043			
Wall018/067			
Wall012/013	0.2614E+04	0.2658E+04	0.2343E+04
Wall012/132			
Wall022/021	0.2484E+04	0.1656E+04	0.1528E+04
Wall022/023			
Wall022/033			
Wall135/136	0.2437E+04	0.2185E+04	0.1922E+04
Wall135/137			
Wall046/047	0.2330E+04	0.1656E+04	0.1528E+04
Wall046/057			
Wall070/071	0.2298E+04	0.1656E+04	0.1528E+04
Wall070/081			

## CONCLUSIONS

In this paper, we used CFD to simulate the flow in a DCU fractionator overhead vapor line connected to an air cooler. The causes of the damage and the strategies of remedying the occurrence of the damage are discussed. It is found that the flow direction of the working fluid in the 30” main pipe biases the downstream flow to the east side, which causes the east half part of the pipe system to deteriorate earlier than the west half part due to the larger erosion effect. Raising the 30” pipe does not improve the force uniformity. If the two 24” pipes are connected and the five 18” pipes are also connected, the force

uniformity can be improved without raising the 30" pipe. In addition, the forces on caps, reducers and T-junctions all reduce if the two 24" pipes are connected and the five 18" pipes are also connected. The results of this study can provide a reference for solving similar DCU pipeline problems.

## REFERENCES

- Abdul Rahman, N., "Steady State Simulation of a Delayed Coker Unit," Bachelor thesis, Universiti Teknologi Petronas (2009).
- Albers, J.E., "Modeling of a Delayed Coker," Master of Science thesis, Texas Tech University (1996).
- ASME BPVC.VIII.1-2023, *MANDATORY APPENDIX 13: VESSELS OF NONCIRCULAR CROSS SECTION*, pp.397-425 (2023).
- Chen, W. and Wang, J., "Effects of Blending Ethylene Tar on Colloidal Stability of Delayed Coker Feedstock and Pyrolysis Process," *Pet. Process. Petchems.*, Vol.35, No.7, pp.61-64 (2020).
- Deng, Z., Cai, G. and Li, Y., "Influence of High Proportion Blending Catalytic Cracking Slurry on Delayed Coker," *Pet. Process. Petchems.*, Vol.58, No.12, pp.8-12 (2022).
- Depew, C.A., Hashemi, M.H. and Davis, J., "Evaluation of Alternative Control Strategies for Delayed Coker by Dynamic Simulation," *Proc. 1988 Am. Control Conf.*, Atlanta, GA, USA, pp.240-246 (1988).
- Díaz, F.A., Chaves-Guerrero, A., Gauthier-Maradei, P., Fuentes, D., Guzmán, A. and Picón, H., "CFD Simulation of a Pilot Plant Delayed Coking Reactor Using an In-House CFD Code," *CTF – Cienc. Tecn. Fut.*, Vol.7, No.1, pp.85-100 (2017).
- Fan, Y., Lu, Q., Wu, Z. and Ma, S., "Intelligent Optimization of Three-Point Steam Injection Rate in Delayed Coker Furnace Based on Automatic Regulation of Heat Load," *Pet. Process. Petchems.*, Vol.51, No.9, pp.86-91 (2022).
- Fluent Inc., *ANSYS FLUENT 17 User's Guide*, Fluent Inc., New York (2017).
- Ge, X., "Technical Analysis of Reprocessing Mixed Waste Oil into Delayed Coker," *Pet. Process. Petchems.*, Vol.58, No.12, pp.13-18 (2022).
- Hsu, C.S. and Robinson, P.R., *Chap.12: Coking and Visbreaking, Petroleum Science and Technology*, ISBN 978-3-030-16275-7 (eBook), Springer Nature, Switzerland (2019).
- Ibrahim, S.A.M., Abdalla, B.K., Mohamed, A.A. and Elbasher, H.A., "Evaluation and Simulation of Different Crude Oil in Delayed Coker Unit (DCU) in Khartoum Refinery," *Eur. Acad. Res.*, Vol.X, No.4, pp.1410-1421 (2022).
- Kedia, V., Nallasivam, U., and Ambati, S.R., "Disturbance Modelling Based Benefit Estimation from Advanced Process Control: Case study on Delayed Coker Unit," *2019 Fifth Indian Control Conf.*, IIT Delhi, India (2019).
- Lauder, B.E. and Spalding, D.B., *Lectures in Mathematical Models of Turbulence*, Academic Press, London (1972).
- Lauder, B.E. and Spalding, D.B., "The Numerical Computation of Turbulent Flows," *Comput. Methods Appl. Mech. Eng.*, Vol.3, No.2, pp.269-289 (1974).
- Lei, Y., Chen, X., Zhang, B. and Chen, Q., "Integrated Optimization of the Fractionation and Heat Exchange Processes in Delayed Coker with Considering Steam Generation," *Acta Petrol. Sin.*, Vol.31, No.2, pp.572-582 (2015).
- Mohamed, S.N., ElSayed N.A., Abdallah, S.M. and ElSokary, M., "Maximize the Gas Oil Yield from Delayed Coker Unit by Optimization between Process Variables," *J. Univ. Shanghai Sci. Technol.*, Vol.24, No.11, pp.95-109 (2022).
- Paladino, E.E., Ribeiro, D., Reis, M.V., Geraldelli, W.O. and Barros, F.C.C., "A CFD Model for the Washing Zone in Coker Fractionators," *2005 AICHE Annu. Meet.*, Cincinnati, Ohio (2005).
- Patankar, S.V., *Numerical Heat Transfer and Fluid Flows*, McGraw-Hill, New York (1980).
- Valenca, P.A., Waturuocha, A. and Wisecarver K., "2D Axisymmetric Temperature Profile Modelling of a Delayed Coking Drum during Pre-run Warm up," *Proc. 2015 COMSOL Conf.*, Boston (2015).
- Zhang, K. and Yu, J., "Modeling Delayed Coking Plant via RBF Neural Networks," *Proc. Int. Jt. Conf. Neural Netw.*, Washington, DC, USA, Vol.5, pp.3483-3486 (1999).

## NOMENCLATURE

- $C_{\mu}$  turbulence model constant  
 $f$  physical variables  
 $\bar{f}$  average of  $f_1, f_2, \dots, f_n$   
 $k$  turbulence kinetic energy  
 $L$  hydraulic diameter  
 $\varepsilon$  turbulence kinetic energy dissipation rate  
 $\gamma$  uniformity index

# 延遲焦化裝置分餾塔頂蒸 汽管線流場數值模擬分析

葉俊郎

國立虎尾科技大學飛機工程系

## 摘要

本研究針對延遲焦化裝置分餾塔頂蒸氣管線流場進行數值模擬分析，研究中探討管線操作時所可能發生之異常問題及其解決方法；研究結果發現，會造成空冷器管線受損程度不均的主因是由於主管線流入五座空冷器時之不對稱性所致，由於30"主管線中的流動方向偏向東側，導致偏東側下游管線磨蝕效應比偏西側下游管線嚴重；將30"管線抬高對於受力均勻度改善效果並不顯著；由受力均勻度及總受力值大小的探討可發現，將兩段24"管連通及五段18"管連通，但30"主管不抬高時，可得到較佳之受力均勻度與較小總受力值。本研究之結果可提供解決DCU管線遭遇類似問題時之參考。